

RESEARCH

Open Access



# A community challenge to predict clinical outcomes after immune checkpoint blockade in non-small cell lung cancer

Mike Mason<sup>1</sup>, Óscar Lapuente-Santana<sup>2†</sup>, Anni S. Halkola<sup>3†</sup>, Wenyu Wang<sup>4†</sup>, Raghvendra Mall<sup>5,6,7†</sup>, Xu Xiao<sup>8,9†</sup>, Jacob Kaufman<sup>10,11†</sup>, Jingxin Fu<sup>12†</sup>, Jacob Pfeil<sup>13†</sup>, Jineta Banerjee<sup>14</sup>, Verena Chung<sup>14</sup>, Han Chang<sup>1</sup>, Scott D. Chasalow<sup>1</sup>, Hung Ying Lin<sup>1</sup>, Rongrong Chai<sup>14</sup>, Thomas Yu<sup>14</sup>, Francesca Finotello<sup>15,16</sup>, Tuomas Mirtti<sup>17,18,19,20</sup>, Mikko I. Mäyränpää<sup>17</sup>, Jie Bao<sup>4</sup>, Emmy W. Verschuren<sup>21</sup>, Eiman I. Ahmed<sup>22</sup>, Michele Ceccarelli<sup>23,24</sup>, Lance D. Miller<sup>25,26</sup>, Gianni Monaco<sup>24</sup>, Wouter R. L. Hendrickx<sup>22,27</sup>, Shamaa Sherif<sup>22,27</sup>, Lin Yang<sup>12</sup>, Ming Tang<sup>12</sup>, Shengqing Stan Gu<sup>12</sup>, Wubing Zhang<sup>12</sup>, Yi Zhang<sup>12</sup>, Zexian Zeng<sup>12</sup>, Avinash Das Sahu<sup>12</sup>, Yang Liu<sup>12†</sup>, Wenxian Yang<sup>28†</sup>, Davide Bedognetti<sup>22,27,29†</sup>, Jing Tang<sup>4,30†</sup>, Federica Eduati<sup>2,31†</sup>, Teemu D. Laajala<sup>3,17,18,19,32,33†</sup>, William J. Geese<sup>1</sup>, Justin Guinney<sup>34†</sup>, Joseph D. Szustakowski<sup>1†</sup>, Benjamin G. Vincent<sup>35†</sup> and David P. Carbone<sup>11\*†</sup> 

## Abstract

**Background** Predictive biomarkers of immune checkpoint inhibitor (ICI) efficacy are currently lacking for non-small cell lung cancer (NSCLC). Here, we describe the results from the Anti-PD-1 Response Prediction DREAM Challenge, a crowdsourced initiative that enabled the assessment of predictive models by using data from two randomized controlled clinical trials (RCTs) of ICIs in first-line metastatic NSCLC.

**Methods** Participants developed and trained models using public resources. These were evaluated with data from the CheckMate 026 trial (NCT02041533), according to the model-to-data paradigm to maintain patient confidentiality. The generalizability of the models with the best predictive performance was assessed using data from the CheckMate 227 trial (NCT02477826). Both trials were phase III RCTs with a chemotherapy control arm, which

<sup>†</sup>Óscar Lapuente-Santana, Anni S. Halkola, Wenyu Wang, Raghvendra Mall, Xu Xiao, Jacob Kaufman, Jingxin Fu and Jacob Pfeil Lead authors from participating teams in the Anti-PD-1 Response Prediction DREAM Challenge with equal contribution.

<sup>†</sup>Yang Liu, Wenxian Yang, Davide Bedognetti, Jing Tang, Federica Eduati and Teemu D. Laajala Senior authors from participating teams in the Anti-PD-1 Response Prediction DREAM Challenge with equal contribution.

<sup>†</sup>Justin Guinney, Joseph D. Szustakowski, Benjamin G. Vincent and David P. Carbone Co-senior authors from the Anti-PD-1 Response Prediction DREAM Challenge steering committee.

\*Correspondence:

David P. Carbone

david.p.carbone@gmail.com

Full list of author information is available at the end of the article



supported the differentiation between predictive and prognostic models. Isolated model containers were evaluated using a bespoke strategy that considered the challenges of handling transcriptome data from clinical trials.

**Results** A total of 59 teams participated, with 417 models submitted. Multiple predictive models, as opposed to a prognostic model, were generated for predicting overall survival, progression-free survival, and progressive disease status with ICIs. Variables within the models submitted by participants included tumor mutational burden (TMB), programmed death ligand 1 (PD-L1) expression, and gene-expression-based signatures. The best-performing models showed improved predictive power over reference variables, including TMB or PD-L1.

**Conclusions** This DREAM Challenge is the first successful attempt to use protected phase III clinical data for a crowdsourced effort towards generating predictive models for ICI clinical outcomes and could serve as a blueprint for similar efforts in other tumor types and disease states, setting a benchmark for future studies aiming to identify biomarkers predictive of ICI efficacy.

**Trial registration:** CheckMate 026; NCT02041533, registered January 22, 2014.

CheckMate 227; NCT02477826, registered June 23, 2015.

**Keywords** Non-small cell lung cancer, Immune checkpoint inhibitor, Programmed death-1, Programmed death ligand 1, Predictive model, Biomarkers, Crowdsourcing

## Background

Immune checkpoint inhibitors (ICIs) have revolutionized cancer treatment, with advanced non-small cell lung cancer (NSCLC) among the tumor types showing longer survival with ICIs than with chemotherapy in multiple treatment lines [1–4]. While ICIs have demonstrated high response rates in some tumor types [5], not all patients with advanced cancer eligible for ICIs respond to them, highlighting the need for biomarkers predictive of their efficacy [6–9].

Multiple biomarkers have been explored as predictors of clinical outcomes, including programmed death ligand 1 (PD-L1) expression and tumor mutational burden (TMB), which are used in clinical practice but are imperfect predictors of ICI response and not standardized across studies [10]. Associations between clinical outcomes with ICIs and certain biomarkers, including immune-related gene expression, gene signatures, and adaptive immune receptor repertoire features (e.g., T-cell-inflamed gene expression, chemokine expression, immunologic constant of rejection [ICR], T-cell receptor repertoire clonality) have been reported [11–16]. However, a comparison of performance of these markers using large, independent validation datasets is lacking. Biomarker studies in NSCLC have been limited by small sample sizes and lack of a chemotherapy control arm, preventing differentiation between prognostic and predictive biomarkers [17–20]. Robust predictive biomarkers will be critical to identify patients most likely to benefit from ICIs and could guide treatment choice and serve as trial stratification factors.

Here, we describe the Anti-PD-1 Response Prediction DREAM Challenge, a crowdsourced initiative that

enabled the assessment of predictive models using data from two randomized clinical trials (RCTs) of first-line ICIs in NSCLC. We used an innovative model-to-data paradigm that enabled broad participation without requiring direct access to restricted data. This approach protected patient confidentiality while mitigating the risk of overfitting, lack of replicability, and irreproducibility [21, 22].

The pioneering design of this Challenge addressed scientific and technical issues that the community has faced in identifying robust predictors of ICI efficacy. The engagement of worldwide researchers using a reference dataset and consistent metrics leveled the playing field and allowed for head-to-head comparisons of model performance. The use of data from large, mature, well-annotated RCTs eliminated, at least partially, the limitations of analyses based on smaller trials, observational studies, or restricted sample cohorts. Metrics using information from both treatment and control arms allow the differentiation of prognostic models from those that are predictive of population-level benefit from ICI therapies. Finally, the combination of closed competitive and open cooperative phases of this Challenge enabled unprecedented collaboration among academic and industry leaders.

## Methods

### Challenge questions

A steering committee, including members from Bristol Myers Squibb, Sage Bionetworks, and oncology physician-scientists, developed clinically relevant questions that could be addressed through the DREAM

**Table 1** Challenge questions and metrics used for performance evaluation [23]

Sub-challenge	Challenge Question	BM	Primary Metric <sup>a</sup> for Performance Evaluation
PFS (Sub-challenge 1)	PFS/OS sub-challenges: Predict response to nivolumab, in terms of PFS/OS, via an immune checkpoint-specific model using clinical, demographic, and gene expression data	PFS/OS Harrel's C-index	DSS BM of PFS/OS between the nivolumab and chemotherapy arms
OS (Sub-challenge 2)			
BOR (Sub-challenge 3)	BOR sub-challenge: Predict which patients will not respond and have a BOR of PD	ROC-AUC	DSS BM of BOR between the nivolumab and chemotherapy arms

*AUC* area under the curve, *BOR* best overall response, *C-index* concordance index, *DSS BM* difference in squared scaled basal metrics, *OS* overall survival, *PD* progressive disease, *PFS* progression-free survival, *ROC* receiver operating characteristic

<sup>a</sup> The computing of the primary metric from the BM is shown in Additional file 1: Fig. S1

Challenge framework. This Challenge comprised three sub-challenges to identify models predictive of progression-free survival (PFS), overall survival (OS), and best overall response (BOR) of progressive disease (PD) with ICI treatment (Table 1) [23].

### Training and validation datasets

The design of the Challenge is summarized in Fig. 1. To protect patient confidentiality, participants could not directly access the evaluation dataset (CheckMate 026), in line with the model-to-data paradigm [21]. Because of the abundance of publicly available datasets, participants were not provided training data, thereby maintaining a large testing dataset. The variables available to participants and details on the training data used for model construction are shown in Additional file 1: Table S1 and Supplementary Methods 1, respectively. Gene-expression-based predictors are shown in Additional file 1: Tables S2 and S3. Participants developed and trained predictive models using publicly available resources, including those referenced on the Challenge website (TIDE resources [24], The Cancer Research Institute's iAtlas [25], and other published data [26]) and other datasets accessible via their institutions. To ensure proper execution of the independently trained models on the embargoed evaluation dataset, a synthetic dataset with the same formatting as the evaluation dataset was available. Participants submitted dockerized models [27] consisting of the model itself plus software components to run the model in the DREAM evaluation infrastructure (Additional file 1: Supplementary Methods 3). This approach supported reproducibility and a platform-independent evaluation of submitted models. Each team could submit different models for each sub-challenge.

The evaluation dataset from CheckMate 026 (NCT02041533) [28] was selected because it was large, contained multimodal data, was well-characterized at the clinical and molecular level, and allowed potential differentiation between predictive and prognostic

models [29]. In CheckMate 026, patients with untreated stage IV or recurrent NSCLC and tumor PD-L1  $\geq 1\%$  were randomized 1:1 to receive nivolumab or platinum-based chemotherapy [28]. Top-performing models identified with CheckMate 026 data were validated on an independent dataset from CheckMate 227 (Part 1) (NCT02477826) in patients with stage IV or recurrent NSCLC [30, 31]. Identification of potential biomarkers of response to nivolumab were protocol-defined exploratory end points in both CheckMate 026 and 227. In CheckMate 227, patients with tumor PD-L1  $\geq 1\%$  (Part 1a) received either nivolumab + ipilimumab, nivolumab monotherapy, or chemotherapy; patients with PD-L1  $< 1\%$  (Part 1b) received either nivolumab + ipilimumab, nivolumab + chemotherapy, or chemotherapy for the first-line treatment of metastatic NSCLC [30, 31]. Top-performing models were validated in the nivolumab + ipilimumab arms of CheckMate 227 in patients with any level of PD-L1 expression, as these arms were part of the successful primary end points of that trial. Baseline characteristics of patients in CheckMate 026 and 227 were published previously (Additional file 1: Tables S4 and S5) [28, 30, 31].

### Assessing model performance

The validation dataset was limited to samples with gene expression data. Challenge models were required to be robust to missing TMB data, and their predictions were checked for valid data format, including type, completeness, and sample matching, prior to assessment of model performance. Performance metrics (Table 1) were designed to identify predictive rather than prognostic models: top-performing models should accurately rank response measures for patients in the ICI arm but not in the chemotherapy arm to reflect a model's capacity to inform a clinical decision in favor of one therapy over another. For the PFS sub-challenge, we computed for each model the Harrell's concordance index (C-index) of PFS and model predictions as a basal metric (BM) calculated in each arm [32]. We used the

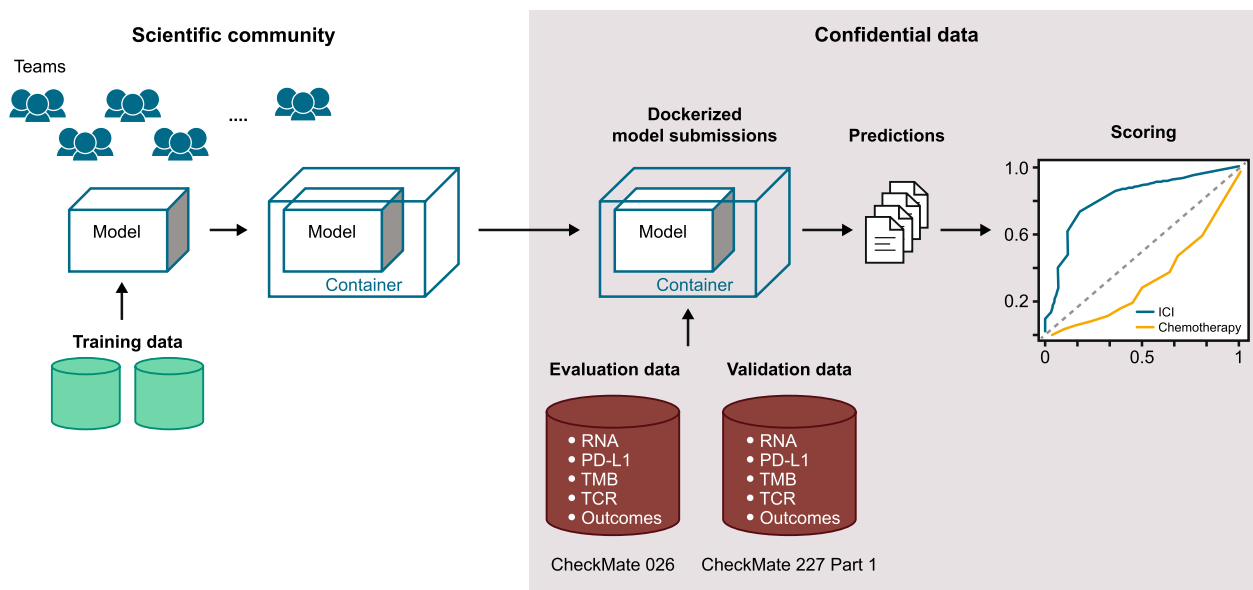


**Fig. 1** Challenge design. *ICI* immune checkpoint inhibitor, *PD-L1* programmed death ligand 1, *TCR* T-cell receptor, *TMB* tumor mutational burden

C-index in the OS sub-challenge after first correcting for potential effects caused by patient crossover from the chemotherapy arm to the nivolumab arm in CheckMate 026 [33]. The C-index was used for the OS and PFS sub-challenges, as it applies to time-to-event outcomes [32]. For the BOR sub-challenge, the BM was the area under the curve (AUC) of the receiver operator curve (ROC) of the model predictions in each arm.

For each sub-challenge, the primary metric applied to each model was the difference in squared scaled BM (DSS) between the nivolumab arm and chemotherapy arm, where  $scaled(BM) = 2 \times (BM - 0.5)$  (Table 1, Additional file 1: Fig. S1) [34, 35]. Models that performed well in the nivolumab arm and randomly in the chemotherapy arm had positive primary scores. Models that performed well in the chemotherapy arm but randomly in the nivolumab arm had negative primary scores. Models that performed the same in each arm had a score of 0. Squaring of the BM allowed us to accommodate models that predicted well in the negative direction as good predictors. A detailed description of the motivation for using DSS and a comparison to other potential metrics are available in Additional file 1: Supplementary Methods 2.

A team’s model performance was determined in each sub-challenge. To be eligible for top-performing status, a model had to outperform the TMB baseline model based on the primary metric (Bayes factor relative to TMB baseline model,  $K_{TMB} > 3$ , see Additional file 1: Supplementary Methods 3). A description of baseline models and published reference models is provided in Additional file 1: Tables S2 and S3. For models meeting

this criterion, we computed  $K_{DSS\_Max}$ , the Bayes factor relative to the highest primary metric in that sub-challenge. Models with  $K_{DSS\_Max} < 3$  were considered tied with the highest scoring model. The BM from the nivolumab arm was used for tie-breaking. If multiple tied models had tie-breaking scores close to the best tie-breaking score, they were included as top-performers for the sub-challenge.

**Results**

**Overall participation in this challenge**

Fifty-one teams and eight individuals made at least one valid submission to the Challenge, with 417 models submitted across the three sub-challenges aiming to identify models predictive of PFS, OS, and BOR of PD with ICI treatment (Table 1) [23]. Top-performing model descriptions are available on the Challenge website (<https://www.synapse.org/#!/Synapse:syn18404605/wiki/609124>), Table 2, and Additional file 1: Supplementary Methods 1. Author teams’ contributions to their respective model are reported in the author teams’ contribution section of Additional file 1. Top-performing models outperformed the 14 comparator models for each sub-challenge.

**Prediction of progression-free survival**

The BM for the PFS sub-challenge was the C-index for observed PFS and model predictions. The primary metric used to determine model performance was the DSS between the nivolumab arm and chemotherapy arm (Table 1).

**Table 2** Description of top-performing models

Model Name	Model Description
Aginome-Amoy Top-performer in the BOR sub-challenge	A rule-based model was generated using patients stratified into three groups based on their PD-L1 and TMB expression scores: Group 1: PD-L1 score below median Group 2: PD-L1 score above median and TMB score below median Group 3: Both PD-L1 and TMB expression scores above median The following heuristic rules were used to decide the ranking of samples: A. Group 3 > Group 1 > Group 2 B. Within Group 3, the ranking of samples was based on the following score: $\text{Score}_{\text{[response]}} = \text{TMB}_{\text{[norm]}} + 2 * \text{PD-L1}_{\text{[norm]}}$ C. Within Group 1, the ranking of samples was based on the following score: $\text{Score}_{\text{[response]}} = \text{TMB}_{\text{[norm]}} + \text{PD-L1}_{\text{[norm]}}$ D. Within Group 2, the ranking of samples was based on the following score: $\text{Score}_{\text{[response]}} = \text{TMB}_{\text{[norm]}} - \text{PD-L1}_{\text{[norm]}}$
cSysImmunoOnco Top-performer in the BOR sub-challenge	A score of immune response was computed for each patient using EaSlER [43], which makes use of elastic-net regularized multitask linear regression models trained on TCGA data using quantitative descriptors of the TME as model input and 10 published transcriptomic signatures of immune response as model output. The quantitative descriptors of the TME included relative abundances of different immune cell types [44], scores of pathway [45] and transcription factor activities [46], and scores of inter-cellular communication and were derived by combining prior knowledge about the tumor microenvironment and patients' transcriptomics data. The models were fine-tuned by associating penalties with markers of tumor foreignness based on TMB, wherever available, or MSI status estimated using an RNA-seq based signature
DukeLKB1 Top-performer in the OS sub-challenge	A model with six derived features (TMB, PD-L1, 4-gene inflammatory signature, <i>LKB1</i> loss signature, <i>NRF2</i> activation signature, and neuroendocrine differentiation signature) was generated [47, 48] The scores included in the model were calculated as follows: for TMB and PD-L1 components, tumors with respective phenotype > 67 <sup>th</sup> percentile were given a score of 1, and remaining tumors were scored 0. The 4-gene inflammatory signature and the three tumor-intrinsic gene expression variables were taken as means of the scaled expression scores for the corresponding signature genes. Because we anticipated differences in gene expression and distribution according to tumor histology, the dataset was first separated into squamous and non-squamous subsets, with scaling and averaging across genes performed separately between the two groups
FICAN-OSCAR Top-performer in the OS sub-challenge	A single linear regression model using a novel <b>Optimal Subset CArdinality Regression</b> ( <i>oscar</i> ) L0-quasinorm regularization was generated using the R package available at <a href="https://github.com/Syksy/oscar/releases/tag/v0.6.1">https://github.com/Syksy/oscar/releases/tag/v0.6.1</a> [49, 50]. The model is a linear product of the data matrix <i>X</i> and regularized beta coefficients <i>b</i> . Gene expression signature (CUSTOM FOPANEL) was estimated using a custom gene panel analyzed with GSVA (with the parameter <i>mx.diff</i> =TRUE). Other variables included in the model were sex, histology (squamous vs. not), smoking history, ECOG performance status (0 vs. not), TMB, and PD-L1. A description of each coefficient is available in Additional file 1: Supplementary Methods 1 FICAN-OSCAR model equation: $Y = -0.693 \times \text{CUSTOM\_FOPANEL} - 0.357 \times \text{isTMBhigh} - 0.105 \times \text{isMale} - 0.198 \times \text{isSquamous} - 0.05 \times \text{isSquamous\&Above5PDL1} - 0.223 \times \text{isEversmoker} - 0.105 \times \text{isECOG0}$
@jacob.pfeil Top-performer in the OS sub-challenge	The AbbVie Taux model used an unbiased feature engineering strategy to identify gene expression ratios that differentiate anti-PD-1 responders from non-responders. The reason for using gene expression ratios was to down-weight the effect of response markers by a factor proportional to resistance marker expression level. Cross-validation and regularization were used to mitigate overfitting on the small number of available training samples. An SVM with radial basis function kernel identified a non-linear boundary separating the responder ratio values from non-responder values. Predictive gene expression ratios balanced markers of response (e.g., immune cell markers, Type-I interferon, HLA presentation) with markers of resistance (e.g., proliferation and inhibitors of immune recognition)

**Table 2** (continued)

Model Name	Model Description
I-MIRACLE Top-performer in the OS sub-challenge	<p>A rule-based prediction model was generated based on classifying TMB and PD-L1 as high or low as follows:</p> <ul style="list-style-type: none"> <li>• TMB: TMB values were classified as high if greater than or equal to the upper tertile and as low otherwise. When TMB was missing, the proliferation score [51] was used as a proxy, as it correlates highly with TMB in NSCLC (see prediction of OS sub-challenge)</li> <li>◦ The proliferation score was calculated for each patient using the yaGST R package (<a href="http://github.com/miccec/yaGST">http://github.com/miccec/yaGST</a>) [52]. Patients with missing TMB were classified as TMB high if their proliferation score was greater than or equal to the upper tertile and as TMB low otherwise</li> <li>• PD-L1: Patients were classified as PD-L1 high if their PD-L1 value was <math>\geq 50</math> and PD-L1 low otherwise. When PD-L1 values were missing, the ICR score was used instead</li> <li>◦ The ICR score was derived from a 20-gene signature that reflects the presence of a Th1/cytotoxic immune response [14, 16]. The ICR score was calculated for all patients using the yaGST R package. Patients with missing PD-L1 were classified as PD-L1 high if their ICR score was greater than or equal to the upper tertile and as PD-L1 low otherwise</li> <li>• Patients were given a I-MIRACLE score of 1, 2, or 3 based on their TMB and PD-L1 values, as shown in Fig. 2B and in Additional file 1: Supplementary Methods 1. If TMB was high (or the proliferation score was high when TMB was missing) and PD-L1 expression was high (or the ICR score was high when PD-L1 was missing), we gave a score of 3. A score of 1 was given when both TMB/proliferation score and PD-L1/ICR were low. A score of 2 was given otherwise</li> </ul>
Netphar Top-performer in the PFS sub-challenge	<p>A decision tree-based model was generated using TMB high (<math>\geq 243</math>) or low (<math>&lt; 243</math>) as a first branching point (prior knowledge: TMB is necessary but not sufficient for triggering the checkpoint inhibitor response) and the expression of PD-L1 in the TMB high branch as the second branching point. The model was designed to be conservative on the TMB low branch with all predictions equal to zero</p> <p>Model equation: <math>Y = 10 \times \text{TMB}_{\text{binarized}} + \text{TMB}_{\text{binarized}} \times \text{PD-L1}</math></p>
Team TIDE Top-performer in the BOR sub-challenge	<p>The model integrated TIDE [24] with other clinical phenotypes (e.g., PD-L1, TMB, and smoking) by the rank aggregation method to enhance the prediction performance on patient survival and response. Treatment-naïve ICI clinical trial data from the TIDE database and late-stage chemotherapy patients of LUAD, LUSC, and SKCM from TCGA were used as the training data. C-index values for survival with each feature within individual cohort and rank features were calculated according to a custom scoring metric. Features such as TMB, PD-L1, CTL, SMOKE, Dysfunction, Exclusion, T.cell.CD4.non.regulatory from QUANTISEQ [44], B-cell naive from xCell [53], IFNG signature, and antigen presentation by MHC-I were selected in the model prediction</p>

*BOR* best overall response, *C-index* concordance index, *CTL* cytotoxic T lymphocytes, *EaSlr* estimate systems immune response, *ECOG* Eastern Cooperative Oncology Group, *GSVA* gene set variation analysis, *HLA* human leukocyte antigen, *ICI* immune checkpoint inhibitor, *ICR* immune constant of rejection, *IFNG* interferon gamma, *LUAD* lung adenocarcinoma, *LUSC* lung squamous cell carcinoma, *MHC-I* major histocompatibility complex I, *MSI* microsatellite instability, *NRF2* nuclear factor erythroid 2-related factor 2, *NSCLC* non-small cell lung cancer, *OS* overall survival, *PD-1* programmed death-1, *PD-L1*, programmed death ligand 1, *PFS* progression-free survival; *RNA-seq*, RNA sequencing; *SKCM*, skin cutaneous melanoma, *SVM* Support Vector Machine, *TCGA* The Cancer Genome Atlas, *TIDE* tumor immune dysfunction and exclusion, *TMB* tumor mutational burden, *TME* tumor microenvironment

In the PFS sub-challenge, the Netphar and I-MIRACLE models outperformed the TMB baseline model, achieving C-index DSS of 0.19 and 0.087, respectively (Fig. 2A). The Netphar model was based on a decision tree positing that high TMB ( $\geq 243$  missense mutations) was necessary but not sufficient to induce a response to nivolumab, and that tumor cell % PD-L1 expression became relevant only when TMB was high (Fig. 2B; Additional file 1: Supplementary Methods 1).

In the nivolumab arm of CheckMate 026, patients with Netphar scores in the upper tertile had longer median PFS (10.8 months) than patients with scores in the middle and lower tertiles (3.5 months), whereas in the chemotherapy arm, patients with scores in the middle and lower tertiles had slightly longer median PFS (7.1 months) than patients with scores in the upper tertile (5.4 months) (Fig. 2C). Netphar scores in the upper tertile were associated with improved median PFS (16.3 months) in the nivolumab + ipilimumab arm of CheckMate 227 compared with scores in the middle and lower tertiles

(2.8 months). In the chemotherapy arm of CheckMate 227, patients with scores in the upper tertile had similar median PFS (5.8 months) to patients with scores in the middle and lower tertiles (4.6 months) (Fig. 2D).

### Prediction of overall survival

The BM for the OS sub-challenge was the C-index for observed OS and model predictions. As for the PFS sub-challenge, the primary metric was DSS between the nivolumab arm and chemotherapy arm (Table 1).

In the OS sub-challenge, three models had higher C-index DSS than baseline models, including TMB and PD-L1, with I-MIRACLE, FICAN-OSCAR, and DukeLKB1 achieving DSS of 0.050, 0.046, and 0.032, respectively (Fig. 3A). Although the @jacob.pfeil model had the highest DSS (0.0721), bootstrapped estimates of performance for that model showed substantial variation.

The I-MIRACLE model gave patients a score of 1, 2, or 3 based on their TMB and PD-L1 values (Fig. 3B and Table 2).

In the nivolumab arm of CheckMate 026, patients with I-MIRACLE scores of 3 had better median OS (not reached) than patients with scores of 2 (14.1 months) or 1 (11.8 months), whereas in the chemotherapy arm, OS was similar in all patients regardless of I-MIRACLE score (15.2, 11.7, 16.9 months with a score of 1, 2, and 3, respectively) (Fig. 3C). In CheckMate 227, I-MIRACLE scores of 3 were associated with prolonged median OS (44.3 months) in the nivolumab+ipilimumab

arm compared with scores of 2 (14.3 months) or 1 (16.7 months). OS was similar in the chemotherapy arm regardless of the score (8.5, 10.7, 12.9 months with a score of 1, 2, and 3, respectively) (Fig. 3D).

**Prediction of best overall response of progressive disease**

The BM for the BOR sub-challenge was the ROC-AUC of the model predictions in each arm, and the primary

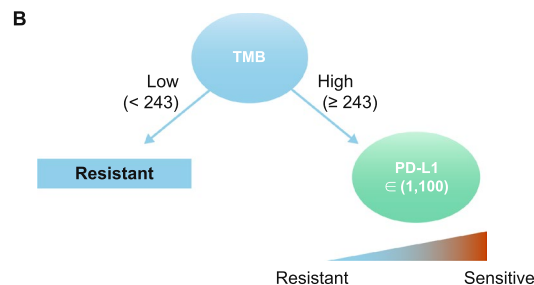
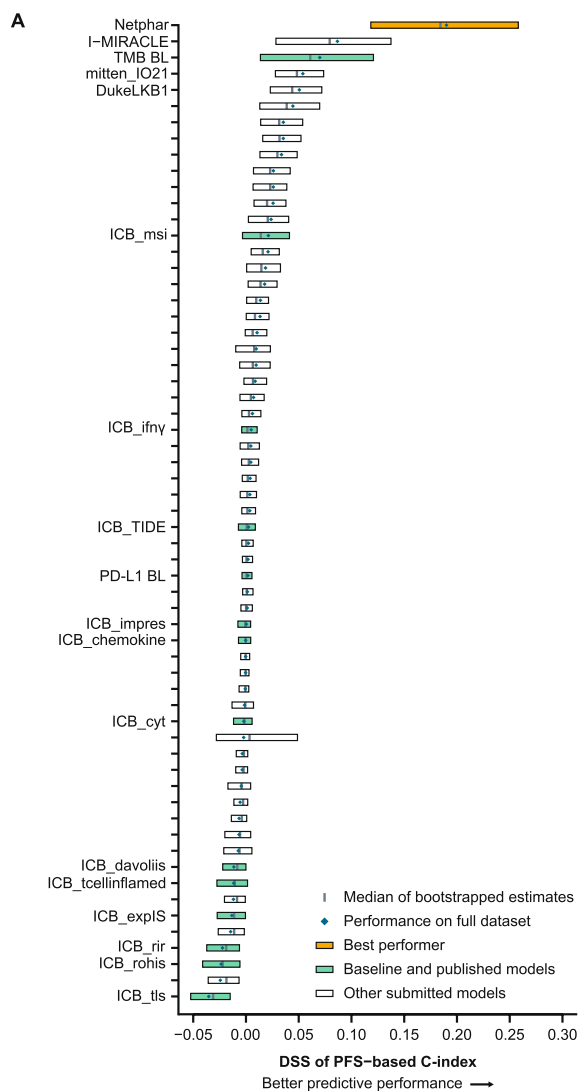


**Fig. 2** Prediction of PFS with submitted models. **A** Bootstrapped estimates of model performance in CheckMate 026 (boxes are bound by the 25th and 75th percentiles). **B** Decision tree summarizing the Netphar model. **C** Netphar performance in the chemotherapy and nivolumab arms of CheckMate 026. **D** Netphar performance in the chemotherapy and nivolumab+ ipilimumab arms of CheckMate 227. *BL* baseline, *C-index* concordance index, *DSS BM* difference in squared scaled basal metrics, *PD-L1* programmed death ligand 1, *PFS* progression-free survival, *TMB* tumor mutational burden

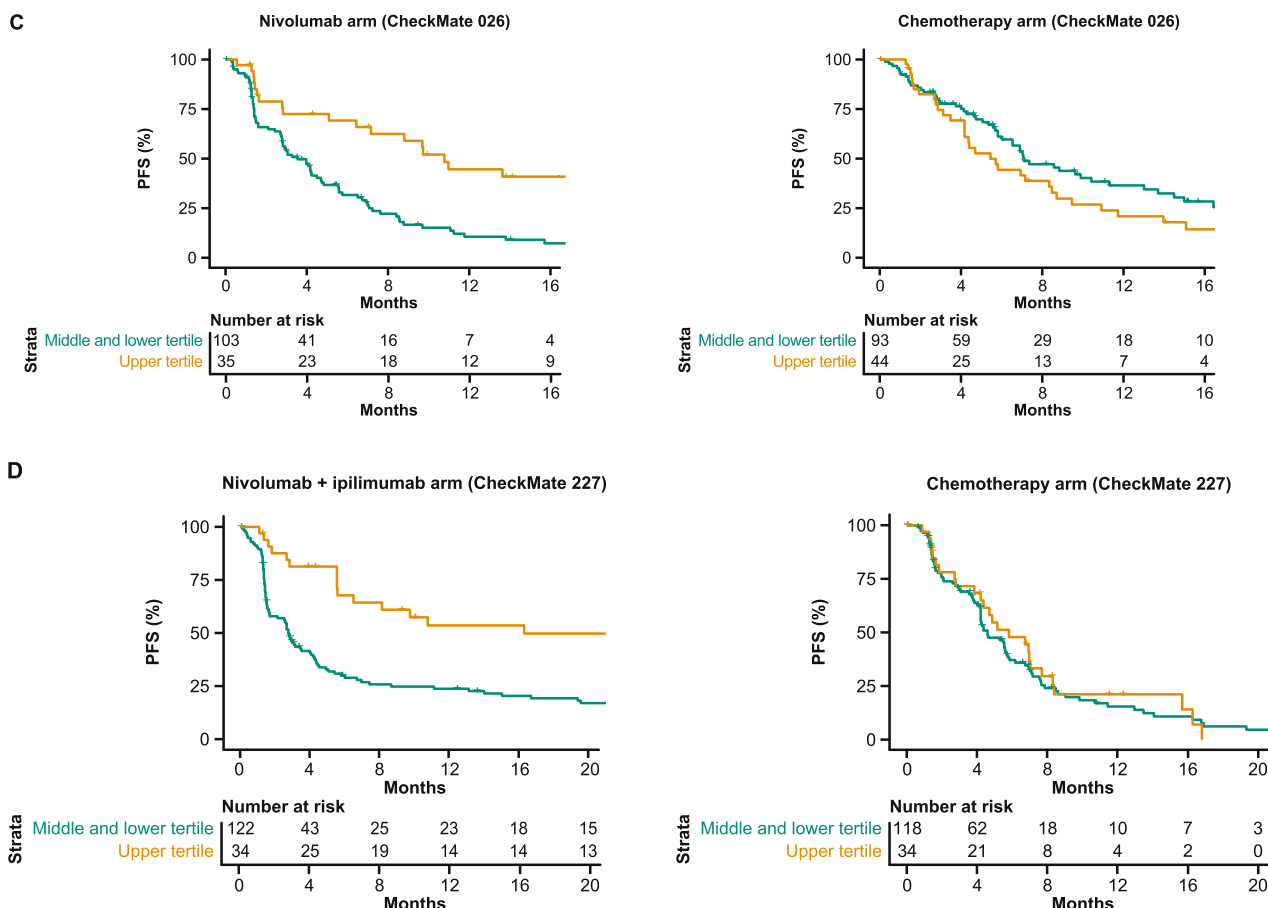


Fig. 2 continued

metric used for model performance was DSS between the nivolumab and chemotherapy arm (Table 1).

Four models in the BOR sub-challenge surpassed the performance of all baseline models. The DSS of ROC-AUC was 0.055 for cSysImmunoOnco, 0.052 for Aginome-Amoy, 0.049 for Team TIDE, and 0.039 for FICAN-OSCAR (Fig. 4A). The cSysImmunoOnco model applied regularized multi-task linear regression to model hallmarks of anticancer immune response based on quantitative descriptors of the tumor microenvironment and TMB (Fig. 4B).

The ROC-AUC with the cSysImmunoOnco model was higher in the nivolumab arm of CheckMate 026 (0.626) and nivolumab + ipilimumab arm of CheckMate 227 (0.593) than in the chemotherapy arm of CheckMate 026 (0.547) or the chemotherapy arm of CheckMate 227 (0.465) (Fig. 4C and D).

**Model performance**

Several models had similar or better performance in CheckMate 227 than in CheckMate 026 (Additional file 1:

Fig. S2). Netphar was the top-performing model for PFS prediction in the nivolumab arm of CheckMate 026 and in the nivolumab + ipilimumab arm of CheckMate 227. The Netphar model had good predictive accuracy for OS in the nivolumab + ipilimumab arm of CheckMate 227. The I-MIRACLE model had good predictive accuracy for PFS in CheckMate 026 (Additional file 1: Table S6). The cSysImmunoOnco model did not have good predictive accuracy for PFS or OS in CheckMate 026.

**Gene signatures**

Multiple teams (cSysImmunoOnco, I-MIRACLE, Team TIDE, and FICAN-OSCAR) leveraged publicly available gene expression data to train the models and deemed the expression of a select assortment of genes important (Additional file 1: Supplementary Methods 4). The Duke-LKB1 six-feature model included a validated transcriptional signature of STK11 functional loss as a predictive feature [36]. Among the models relying on gene expression information, the cSysImmunoOnco model used the expression of > 100 genes, whereas FICAN-OSCAR

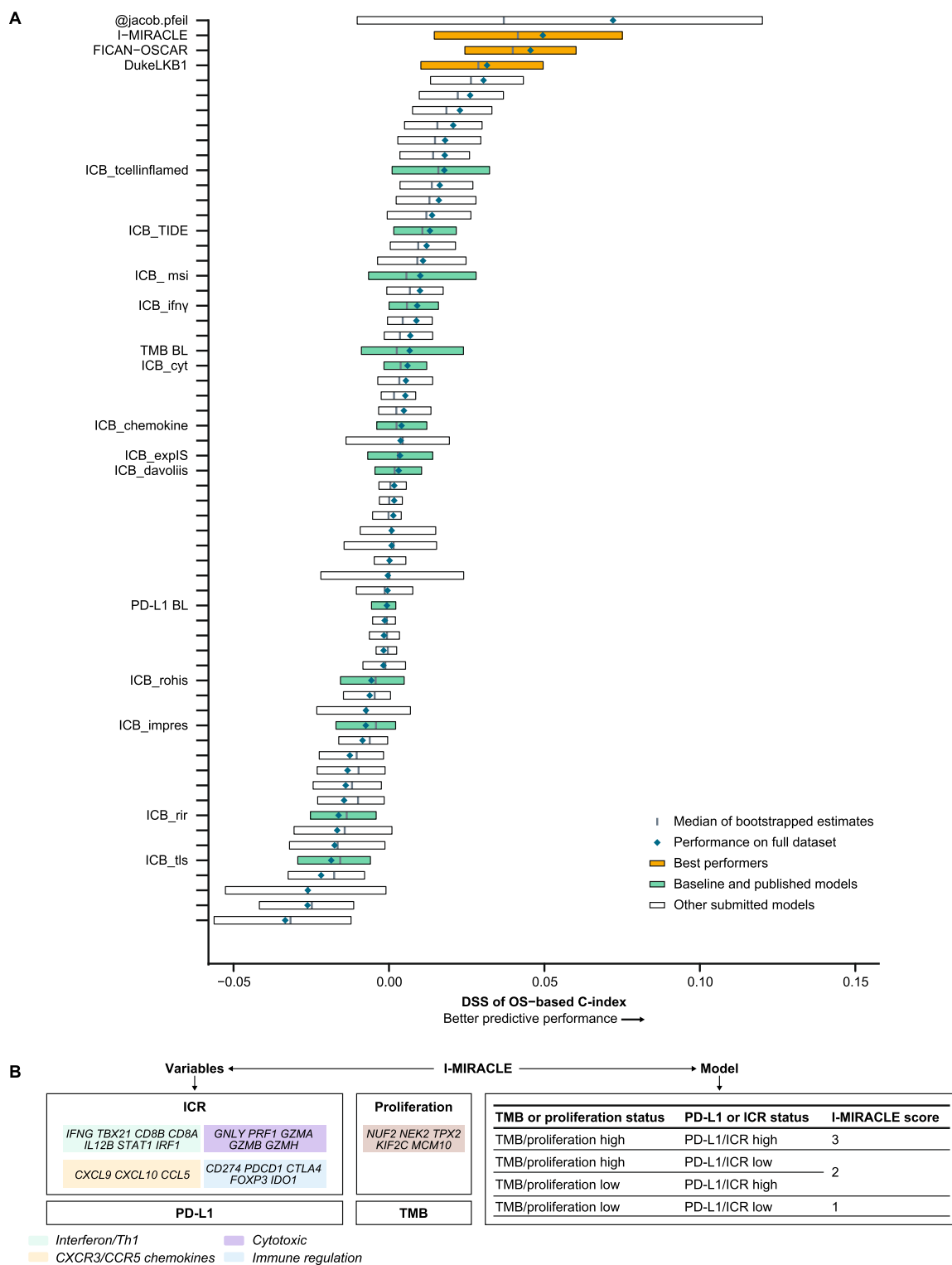


**Fig. 3** Prediction of OS with submitted models. **A** Bootstrapped estimates of model performance in CheckMate 026 (Boxes are bound by the 25th and 75th percentile). **B** Classification principle of the I-MIRACLE model. **C** I-MIRACLE performance in the chemotherapy and nivolumab arms of CheckMate 026. **D** I-MIRACLE performance in the chemotherapy and nivolumab + ipilimumab arms of CheckMate 227. *BL* baseline, *C-index* concordance index, *DSS BM* difference in squared scaled basal metrics, *ICR* immunologic constant of rejection, *OS* overall survival, *PD-L1* programmed death ligand 1, *PFS* progression-free survival, *TMB* tumor mutational burden

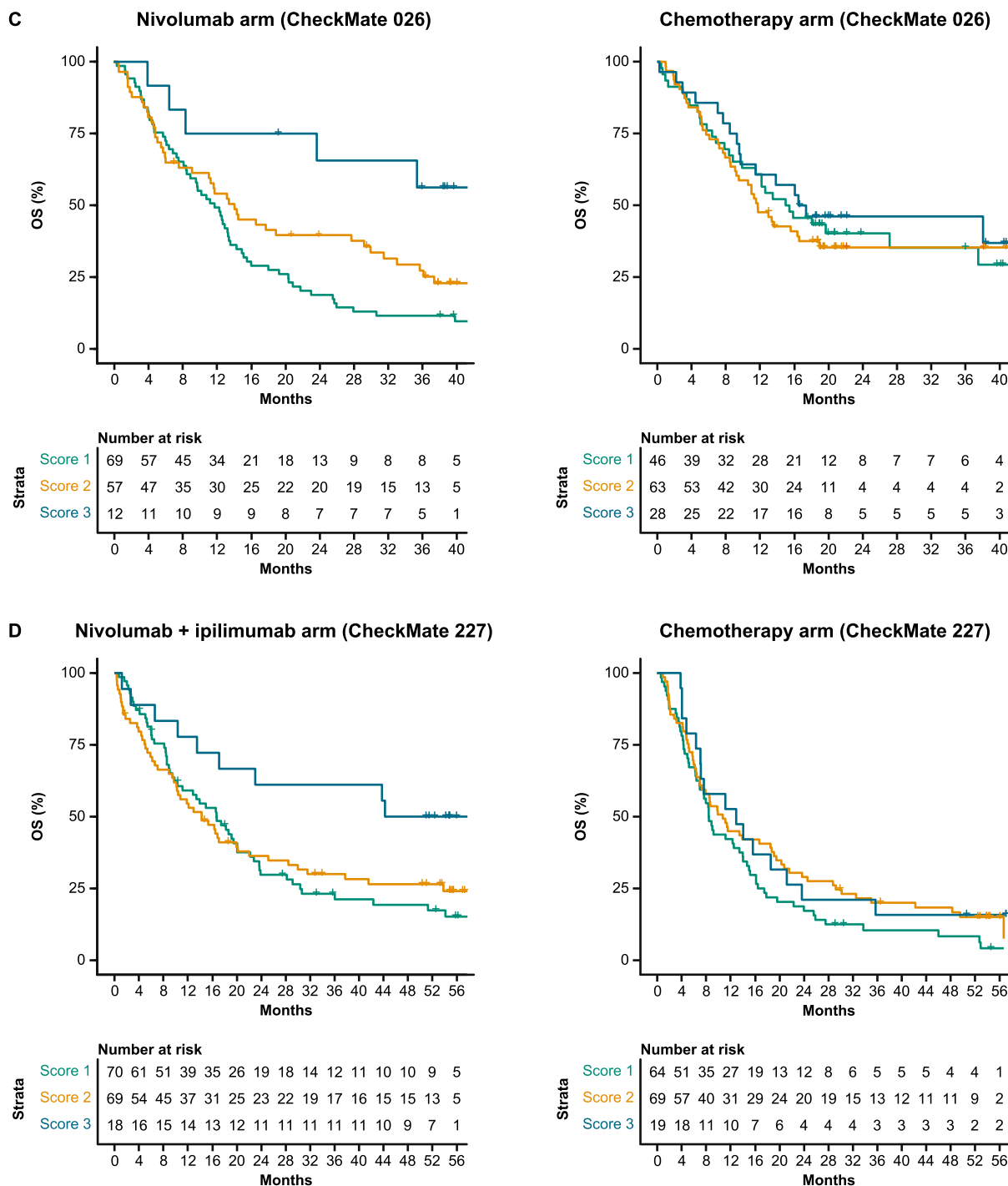
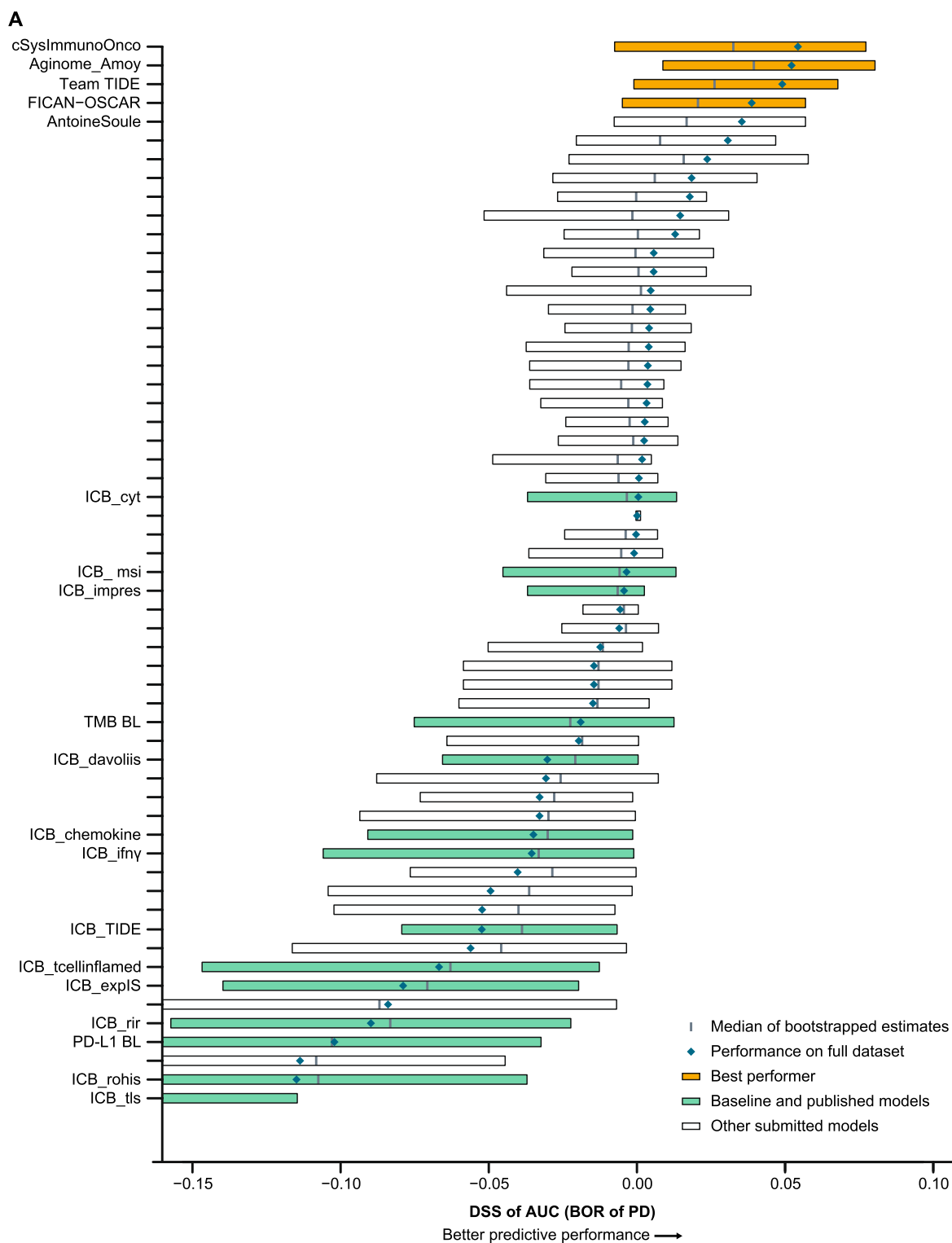


Fig. 3 continued

relied on five genes (Additional file 1: Fig. S3A). A total of 140 genes ranked important by various models were selected as seeds for downstream analysis. Additional

genes that were highly correlated to the seed genes (correlation > 0.85) were included to form a set of 403 genes grouped into three clusters using hierarchical clustering



**Fig. 4** Prediction of BOR of PD with submitted models. **A** Bootstrapped estimates of model performance in CheckMate 026 (boxes are bound by the 25th and 75th percentiles). **B** Principle of the cSysImmunoOnco model. **C** cSysImmunoOnco model performance in CheckMate 026 and **D** CheckMate 227. The grey dotted line is the line of non-determination. *AUC* area under the curve, *BL* baseline, *BOR* best overall response, *DSS BM* difference in squared scaled basal metrics, *EaSlER* estimate systems immune response, *ICI* immune checkpoint inhibitor, *ICR* immunologic constant of rejection, *MSI* microsatellite instability, *NSCLC* non-small cell lung cancer, *OS* overall survival, *PD* progressive disease, *PD-L1* programmed death ligand 1, *TMB* tumor mutational burden

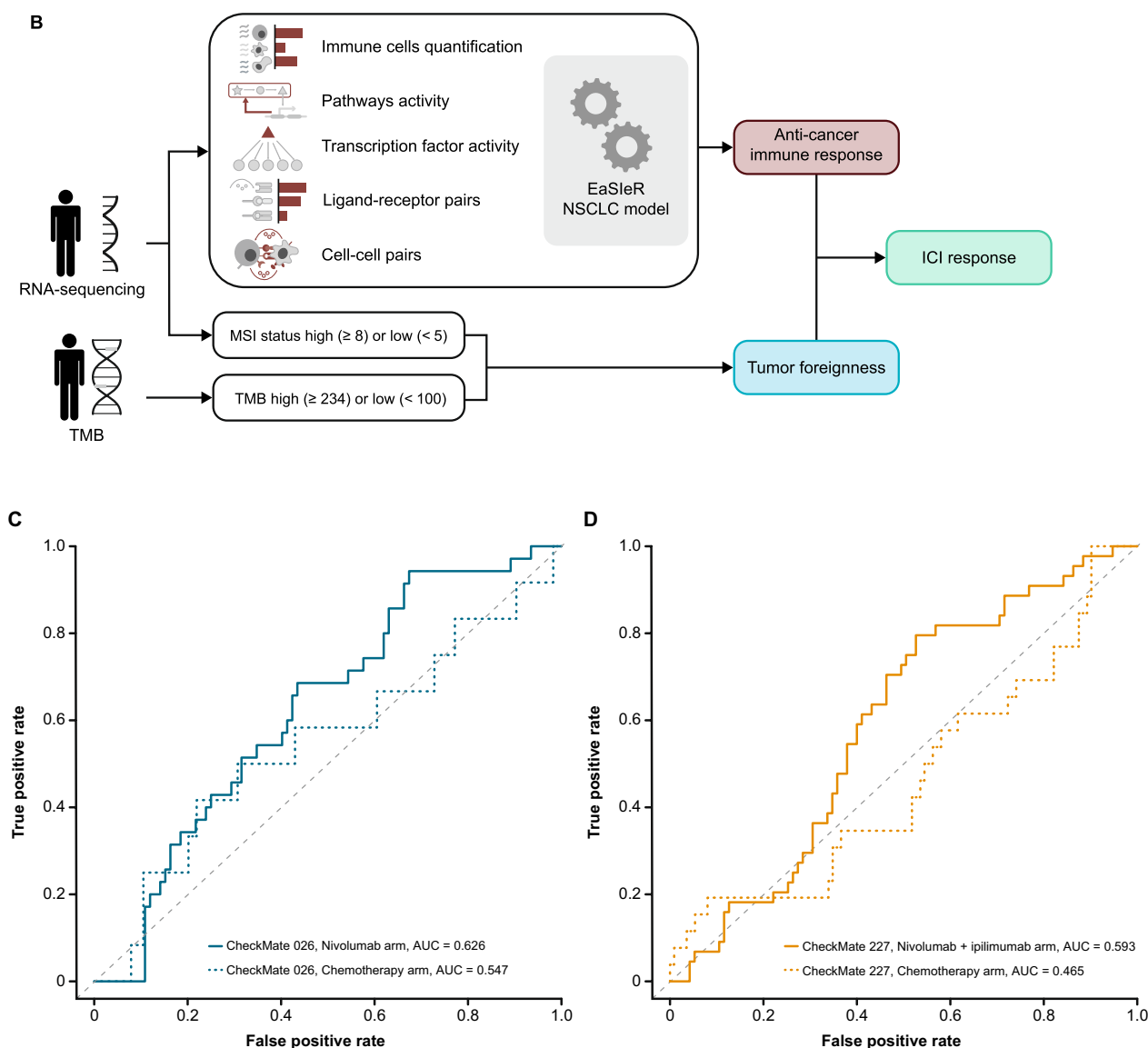


Fig. 4 continued

(Additional file 1: Fig. S3B). Analysis of the three clusters showed the enrichment of three main mechanisms. The first cluster represented pathways relevant to tumor intrinsic cell-cycle dysregulation (Additional file 1: Fig. S3Ci, Di). The second cluster included pro-inflammatory immune signatures related to interferon-gamma signaling and antigen presentation (Additional file 1: Fig. S3Cii, Dii). The third cluster included immunosuppressive signatures related to interleukin-10 signaling. The *P* values associated with the third cluster were not small, suggesting weak enrichment, likely due to the small cluster size (Additional file 1: Fig. S3Ciii, Diii). These results show an association of the top predictive genes from the benchmarked models with well-established pathways

related to cell-cycle dysregulation and pro-inflammatory immune response.

**Discussion**

Not all patients with NSCLC achieve a response with ICIs. Consequently, there is a strong need for predictive biomarkers of outcomes with ICIs [9]. Studies reporting associations with ICI response in NSCLC have been limited by small sample sizes from single ICI treatment arms [17, 19, 20]. This Challenge addressed these shortcomings by using two large and well-characterized phase III RCTs and by comparing predicted responses between ICI- and chemotherapy-treated arms, thereby distinguishing treatment response prediction from

prognostic effects. The model-to-data framework was an important characteristic of this Challenge. While participants received limited feedback with this paradigm during model development, which prevented model refinement, this ensured an unbiased and reproducible assessment of the Challenge models [21]. The model-to-data framework could be made accessible to support evaluation of *in silico* predictors using various datasets while maintaining data privacy. This study established a robust standard for researchers aiming to identify biomarkers predictive of ICI efficacy. We expect that future Challenges will support efficient biomarker discovery across multiple contexts.

Participants integrated prior knowledge of ICIs with modeling methods like decision trees and regularized regression, additive models with hand-crafted weights, and decision trees with additive models. Preliminary attempts to aggregate models did not show improvements over individual models. While submitted models significantly outperformed TMB and PD-L1 as univariate predictors, most of the top-performing models included both variables, sometimes combined with gene expression signatures such as ICR or a proliferation signature, which reflected the clinical importance of TMB and PD-L1. This aligns with the observations obtained in tumor types, including head and neck squamous cell carcinoma (HNSCC) and melanoma, in which a T-cell-inflamed gene expression profile (similar to ICR) and TMB predicted PFS in patients receiving pembrolizumab [11]. Likewise, a combined assessment of TMB and an inflammatory signature predicted BOR, PFS, and OS in patients with advanced melanoma receiving nivolumab or nivolumab + ipilimumab [37]. A high ICR score predicted survival or response in patients with multiple tumor types treated with ICIs [14, 16].

These results indicate that a combination of PD-L1, TMB, and immune gene signatures might be able to identify a subgroup of patients with NSCLC likely to respond to ICIs and could be used for the design of a prospective phase III trial or to guide treatment choice. There is no single ‘magic bullet’ biomarker or model-building approach to predict response to ICIs. The biomarker content of top-performing models, as well as the exploration of their gene signature content, reinforce the need to assess tumor biology, tumor immunogenicity, and immune system status to identify patients most likely to benefit from ICI treatment. However, top-performing models differed across sub-challenges, suggesting that composite models have different predictive potential, depending on the clinical end point assessed. For example, TMB and PD-L1 seem important for the prediction of PFS and OS, confirming previous studies

[38], while mechanisms such as apoptosis, T-cell cross talk, and adaptive immune resistance seem important for the prediction of response. Future precision medicine approaches will benefit from the exploration and development of targeted composite biomarker strategies.

The models identified may be generalizable to ICI datasets other than first-line treatment in metastatic NSCLC. Contributing teams used training datasets from other tumor types (melanoma or HNSCC), and the top-performing models in CheckMate 026 were validated in CheckMate 227 with different primary end points. These observations suggest that this approach may provide a blueprint to support modeling initiatives in diverse tumor types. The performance of the Netphar model in the evaluation dataset of CheckMate 026 is not surprising and aligns with the fact that the coefficients of the Netphar model were based on the summary statistics of Checkmate 026 data. However, the Netphar model was validated in the external CheckMate 227 dataset, which confirmed its predictive accuracy.

A possible limitation of this study is that TMB, frequently used in the submitted models, may be inferred from DNA or RNA sequencing data and is a proxy for tumor ‘foreignness’ but does not capture neoantigen clonality and abundance or non-canonical neoantigens generated from other tumor aberrations [39, 40]. Data such as T-cell/B-cell receptor repertoire, tobacco use, Eastern Cooperative Oncology Group (ECOG) performance status, age, and sex are not readily available in public datasets; therefore, participants did not always use them, and their role in predicting response to ICIs needs to be explored further. NSCLC is a genetically heterogeneous disease [41], and specific subpopulations may differ in optimal biomarkers predictive of therapy response. While transcriptional signatures predictive of functional STK11 and KEAP1/NFE2L2 alterations were used in some models, integration of transcriptional phenotypes with fuller exome datasets across larger cohorts will be necessary to discover these subtype-specific biomarkers. Other limitations were the similarity of PFS and OS between the nivolumab and chemotherapy treatment groups of CheckMate 026, and the exclusion of patients with PD-L1 expression <1% in CheckMate 026. Although clinical and molecular data sets from both trials are large and rich, ascertainment of genomics data was incomplete because of logistical limitations. When the CheckMate 026 and 227 studies were conducted, chemotherapy was the standard of care; the current standard is chemotherapy plus ICI [42]. The models identified here should be tested in the context of this new standard.

## Conclusions

This pioneering study showed that a crowdsourced approach could successfully identify clinical and translational characteristics predictive of ICI efficacy. This analysis improves the understanding of the mechanisms of tumor sensitivity and resistance to treatment, which will support the development of therapies for patient subpopulations unlikely to benefit from current ICI regimens. As the methods for measuring TMB and PD-L1 are becoming established, the models identified herein could be easily used for patient stratification in a prospective clinical trial and in clinical practice once validated.

The study provides a roadmap for successful partnership between academic and industry scientists that allows for robust, reproducible biomarker testing while protecting patient data and incentivizing collaboration. We hope that the DREAM Challenge framework will be used to analyze data from many phase III trials, to speed the development of clinically actionable biomarkers and improve patient outcomes.

## Abbreviations

AUC	Area under the curve
BM	Basal metric
BOR	Best overall response
C-index	Harrell's concordance index
DSS	Difference in squared scaled
ECOG	Eastern Cooperative Oncology Group
HNSCC	Head and neck squamous cell carcinoma
ICI	Immune checkpoint inhibitor
ICR	Immunologic constant of rejection
NSCLC	Non-small cell lung cancer
OS	Overall survival
PD	Progressive disease
PD-L1	Programmed death ligand 1
PFS	Progression-free survival
RCT	Randomized clinical trial
ROC	Receiver operator curve
TMB	Tumor mutational burden

## Supplementary Information

The online version contains supplementary material available at <https://doi.org/10.1186/s12967-023-04705-3>.

**Additional file 1: Supplementary Methods 1.** Methods used for the development of best-performing models. **Supplementary Methods 2.** Rationale for metrics used to evaluate model performance. **Supplementary Methods 3.** Model submission by participants and model evaluation. **Supplementary Methods 4.** Pathway analysis of gene sets. **Table S1.** Candidate predictors available to participating teams. **Table S2.** Comparator models: Published and baseline models used for benchmarking. **Table S3.** Components of the published gene signatures detailed in Table S2. **Table S4.** Characteristics at baseline of all the patients who underwent randomization in CheckMate 026. **Table S5.** Characteristics at baseline of all the patients who underwent randomization in CheckMate 227. **Table S6.** Model performance across sub-challenges. **Fig. S1.** Computing of the primary metric for each sub-challenge. **Fig. S2.** Model performance. **Fig. S3.** Gene signatures.

## Acknowledgements

Xiaole Shirley Liu contributed to the development of the TIDE model. Josue Samayoa contributed to the development of the @jacob.pfeil model.

Abraham Apfel contributed data analysis advice. Medical writing and editorial support were provided by Thierry Deltheil, PhD, and Matthew Weddig of Spark Medica Inc., funded by Bristol Myers Squibb.

## Previous presentation

Results from this study have been presented, in part, at the 14th annual RECOMB/ISCB Conference on Regulatory and Systems Genomics with DREAM Challenges (RSGDREAM 2022), November 8–9, 2022, Las Vegas, Nevada, USA.

## Author contributions

MM, WJG, JG, JDS, BGV, DPC: conceptualization, methodology, validation, formal analysis, investigation, writing – review and editing, visualization, supervision. JB, VC, HC, SDC, HYL, RC, TU: methodology, formal analysis, investigation, resources, writing – review and editing. OL-S, ASH, WW, RM, XX, JK, JF, JP, FF, TM, MIM, JB, EWV, EIA, MC, LDM, GM, WRLH, SS, LY, MT, SSG, WZ, YZ, ZZ, ADS, YL, WY, DB, JT, FE, TDL: methodology, formal analysis, investigation, writing – review and editing. All authors read and approved the final manuscript.

## Funding

TDL was funded by the Finnish Cancer Institute and the Finnish Cultural Foundation as a FICAN Cancer Researcher. ASH received funding from the University of Turku Graduate School (MATTI), the Academy of Finland (grants 310507, 313267, and 326238), the Cancer Society of Finland, and the Sigrid Jusélius Foundation. MIM received funding from the Finnish Medical Foundation. TM received funding from the Academy of Finland. FF was supported by the Austrian Science Fund (FWF) [T 974-B30] and the Oesterreichische Nationalbank (OeNB) [18496]. OL-S was supported by the Department of Biomedical Engineering, Eindhoven University of Technology. WW, JB, and JT were supported by an ERC Starting Grant (DrugComb, No. 716063), the Academy of Finland (No. 317680), and the Sigrid Jusélius Foundation. WW was funded by the FIMM-EMBL International PhD programme, Doctoral Programme of Biomedicine at the University of Helsinki, Cancer Foundation Finland, K. Albin Johanssons stiftelse, Ida Montinin Säätiö, Orion Research Foundation sr, and Biomedicum Helsinki Foundation. EV was supported by the Academy of Finland (No. 328437), the iCAN Digital Precision Cancer Medicine Flagship (No. 320185 Academy of Finland), and the CAN-PRO Translational Cancer Medicine Research Program Unit. Data analysis resources were provided by the CSC – IT Center for Science, Finland. JK received funding from the Department of Defense (Lung Cancer Research Program Concept Award LC180633) and was the recipient of a SITC-AstraZeneca Lung Cancer Clinical Fellowship (SPS256666). LY and YL received PACT funding through FNIH. MT received funding from the NIH. SSG was the recipient of the Sara Elizabeth O'Brien Trust Fellowship. ADS received funding from the NCI (K99CA248953) and the Human Immunome Project (MP19-02–190). DB received a grant from the Sidra Medicine Internal Funds (SDR400123). MC received the following grant from AIRC: IG 2018 ID 21846. The study was supported by Bristol Myers Squibb.

## Availability of data and materials

More information on Bristol Myers Squibb's data sharing policy can be found here: <https://www.bms.com/researchers-and-partners/clinical-trials-and-research/disclosure-commitment.html>

## Declarations

### Ethics approval and consent to participate

Not applicable.

### Consent for publication

Not applicable.

### Competing interests

MM, HC, and HYL are employees of Bristol Myers Squibb. MIM has received lecture and/or advisory board fees from Boehringer Ingelheim, Bristol Myers Squibb, MSD, Takeda, Bayer, Amgen, Roche, and Aiforia Technologies Oy. WY is a shareholder of Aginome Scientific. JG is an employee of Tempus Labs. SSG is the recipient of a fellowship from the Sara Elizabeth O'Brien Trust. JS, SC, and WJG are employees and shareholders of Bristol Myers Squibb. BGV received consulting fees from GeneCentric Therapeutics. DPC has received advisory board fees, consulting fees, presentation fees, or consulting fees from Regeneron, Novartis, AbbVie, AstraZeneca, Bristol Myers Squibb, Roche, Arcus

Biosciences, Mirati, Iovance Biotherapeutics, Pfizer, Onc Live, InThought, Glaxo-Smith Kline, Intellisphere, Sanofi, Merck KGaA, Merck/EMD Serono, Johnson & Johnson, Jazz, Janssen, Curio Science, PDD development, G1 Therapeutics, OncoHost, Eisai, Flame Biosciences, Novocure, Merck, Daiichi Sankyo, and Boehringer Ingelheim. Other authors declare that they do not have competing interests.

#### Author details

<sup>1</sup>Bristol Myers Squibb, Princeton, NJ, USA. <sup>2</sup>Department of Biomedical Engineering, Eindhoven University of Technology, Eindhoven, The Netherlands. <sup>3</sup>Department of Mathematics and Statistics, University of Turku, Turku, Finland. <sup>4</sup>Faculty of Medicine, Research Program in Systems Oncology, University of Helsinki, Helsinki, Finland. <sup>5</sup>Qatar Computing Research Institute, Hamad Bin Khalifa University, P.O. Box 34110, Doha, Qatar. <sup>6</sup>Department of Immunology, St. Jude Children's Research Hospital, P.O. Box 38105, Memphis, TN, USA. <sup>7</sup>Biotechnology Research Center, Technology Innovation Institute, P.O. Box 9639, Abu Dhabi, United Arab Emirates. <sup>8</sup>School of Informatics, Xiamen University, Xiamen, China. <sup>9</sup>National Institute for Data Science in Health and Medicine, Xiamen University, Xiamen, China. <sup>10</sup>Department of Medicine, Duke University, Durham, NC, USA. <sup>11</sup>The Ohio State University Comprehensive Cancer Center, Columbus, OH, USA. <sup>12</sup>Dana-Farber Cancer Institute, Boston, MA, USA. <sup>13</sup>AbbVie, South San Francisco, CA, USA. <sup>14</sup>Sage Bionetworks, Seattle, WA, USA. <sup>15</sup>Institute of Molecular Biology, University of Innsbruck, Innsbruck, Austria. <sup>16</sup>Digital Science Center (DiSC), University of Innsbruck, Innsbruck, Austria. <sup>17</sup>Department of Pathology, University of Helsinki and Helsinki University Hospital, Helsinki, Finland. <sup>18</sup>Research Program in Systems Oncology, University of Helsinki, Helsinki, Finland. <sup>19</sup>iCAN-Digital Precision Cancer Medicine Flagship, Helsinki, Finland. <sup>20</sup>Department of Biomedical Engineering, School of Medicine, Emory University, Atlanta, GA, USA. <sup>21</sup>Institute for Molecular Medicine Finland (FIMM), HiLIFE, University of Helsinki, Helsinki, Finland. <sup>22</sup>Human Immunology Department, Sidra Medicine, P.O. Box 26999, Doha, Qatar. <sup>23</sup>Department of Electrical Engineering and Information Technology (DIETI), University of Naples "Federico II", 80125 Naples, Italy. <sup>24</sup>BIOGEM Institute of Molecular Biology and Genetics, Via Camporeale, Ariano Irpino, Italy. <sup>25</sup>Department of Cancer Biology, Wake Forest School of Medicine, Winston-Salem, NC, USA. <sup>26</sup>Atrium Health Wake Forest Baptist Comprehensive Cancer Center, Winston-Salem, NC, USA. <sup>27</sup>College of Health and Life Sciences, Hamad Bin Khalifa University, P.O. Box 26999, Doha, Qatar. <sup>28</sup>Aginome Scientific, Xiamen, China. <sup>29</sup>Department of Internal Medicine and Medical Specialties, University of Genoa, Genoa, Italy. <sup>30</sup>Department of Biochemistry and Developmental Biology, Faculty of Medicine, University of Helsinki, Helsinki, Finland. <sup>31</sup>Institute for Complex Molecular Systems (ICMS), Eindhoven University of Technology, Eindhoven, The Netherlands. <sup>32</sup>FICAN West Cancer Centre, University of Turku and Turku University Hospital, Turku, Finland. <sup>33</sup>Department of Pharmacology, Anschutz Medical Campus, University of Colorado, Denver, CO, USA. <sup>34</sup>Tempus Labs, Chicago, IL, USA. <sup>35</sup>Department of Medicine, Division of Hematology, Department of Microbiology and Immunology, Curriculum in Bioinformatics and Computational Biology, Computational Medicine Program, University of North Carolina at Chapel Hill, Chapel Hill, NC, USA.

Received: 24 October 2023 Accepted: 5 November 2023

Published: 21 February 2024

#### References

1. Antonia SJ, Borghaei H, Ramalingam SS, et al. Four-year survival with nivolumab in patients with previously treated advanced non-small-cell lung cancer: a pooled analysis. *Lancet Oncol.* 2019;20(10):1395–408.
2. Herbst RS, Giaccone G, de Marinis F, et al. Atezolizumab for first-line treatment of PD-L1-selected patients with NSCLC. *N Engl J Med.* 2020;383(14):1328–39.
3. Reck M, Rodriguez-Abreu D, Robinson AG, et al. Pembrolizumab versus chemotherapy for PD-L1-positive non-small-cell lung cancer. *N Engl J Med.* 2016;375(19):1823–33.
4. Borghaei H, Gettinger S, Vokes EE, et al. Five-year outcomes from the randomized, phase III trials CheckMate 017 and 057: Nivolumab versus docetaxel in previously treated non-small-cell lung cancer. *J Clin Oncol.* 2021;39(7):723–33.
5. Cerceak A, Lumish M, Sinopoli J, et al. PD-1 blockade in mismatch repair-deficient, locally advanced rectal cancer. *N Engl J Med.* 2022;386(25):2363–76.
6. Li J, He Q, Yu X, Khan K, Weng X, Guan M. Complete response associated with immune checkpoint inhibitors in advanced non-small-cell lung cancer: a meta-analysis of nine randomized controlled trials. *Cancer Manag Res.* 2019;11:1623–9.
7. Pu X, Wu L, Su D, Mao W, Fang B. Immunotherapy for non-small cell lung cancers: biomarkers for predicting responses and strategies to overcome resistance. *BMC Cancer.* 2018;18(1):1082.
8. Haslam A, Prasad V. Estimation of the percentage of US patients with cancer who are eligible for and respond to checkpoint inhibitor immunotherapy drugs. *JAMA Netw Open.* 2019;2(5):e192535–635.
9. Cancer immunotherapy: the quest for better biomarkers. *Nat Med.* 2022;28:2437.
10. Truesdell J, Miller VA, Fabrizio D. Approach to evaluating tumor mutational burden in routine clinical practice. *Transl Lung Cancer Res.* 2018;7(6):678–81.
11. Cristescu R, Mogg R, Ayers M, et al. Pan-tumor genomic biomarkers for PD-1 checkpoint blockade-based immunotherapy. *Science.* 2018;362(6411):3593.
12. Litchfield K, Reading JL, Puttick C, et al. Meta-analysis of tumor- and T cell-intrinsic mechanisms of sensitization to checkpoint inhibition. *Cell.* 2021;184(3):596–614.e14.
13. Duan Q, Zhang H, Zheng J, Zhang L. Turning cold into hot: Firing up the tumor microenvironment. *Trends Cancer.* 2020;6(7):605–18.
14. Roelands J, Hendrickx W, Zoppoli G, et al. Oncogenic states dictate the prognostic and predictive connotations of intratumoral immune response. *J Immunother Cancer.* 2020;8(1):e000617.
15. Bortone DS, Woodcock MG, Parker JS, Vincent BG. Improved T-cell receptor diversity estimates associate with survival and response to anti-PD-1 therapy. *Cancer Immunol Res.* 2021;9(1):103–12.
16. Roelands J, Kuppen PJK, Ahmed EI, et al. An integrated tumor, immune and microbiome atlas of colon cancer. *Nat Med.* 2023;29(5):1273–86.
17. Cho J-W, Hong MH, Ha S-J, et al. Genome-wide identification of differentially methylated promoters and enhancers associated with response to anti-PD-1 therapy in non-small cell lung cancer. *Exp Mol Med.* 2020;52(9):1550–63.
18. Hwang S, Kwon A-Y, Jeong J-Y, et al. Immune gene signatures for predicting durable clinical benefit of anti-PD-1 immunotherapy in patients with non-small cell lung cancer. *Sci Rep.* 2020;10(1):643.
19. Prat A, Navarro A, Paré L, et al. Immune-related gene expression profiling after PD-1 blockade in non-small cell lung carcinoma, head and neck squamous cell carcinoma, and melanoma. *Cancer Res.* 2017;77(13):3540–50.
20. Jung H, Kim HS, Kim JY, et al. DNA methylation loss promotes immune evasion of tumours with high mutation and copy number load. *Nat Commun.* 2019;10(1):4278.
21. Guinney J, Saez-Rodriguez J. Alternative models for sharing confidential biomedical data. *Nat Biotechnol.* 2018;36(5):391–2.
22. Bentzen SM, Constine LS, Deasy JO, et al. Quantitative analyses of normal tissue effects in the clinic (QUANTEC): an introduction to the scientific issues. *Int J Radiat Oncol Biol Phys.* 2010;76(3 Suppl):S3–9.
23. Vincent BG, Szustakowski JD, Doshi P, Mason M, Guinney J, Carbone DP. Pursuing better biomarkers for immunotherapy response in cancer through a crowdsourced data challenge. *JCO Precis Oncol.* 2021;5:51–4.
24. Fu J, Li K, Zhang W, et al. Large-scale public data reuse to model immunotherapy response and resistance. *Genome Med.* 2020;12(1):21.
25. Eddy JA, Thorsson V, Lamb AE, et al. CRI iAtlas: an interactive portal for immuno-oncology research. *F1000Res.* 2020;9:1028.
26. Synapse. Anti-PD1 response prediction DREAM challenge. 2021. <https://www.synapse.org/#Synapse:syn18404605/wiki/607227>. Nov 2021.
27. Merkel D. Docker: lightweight Linux containers for consistent development and deployment. *Linux J.* 2014. <https://doi.org/10.1056/NEJMoa1613493>.
28. Carbone DP, Reck M, Paz-Ares L, et al. First-line nivolumab in stage IV or recurrent non-small-cell lung cancer. *N Engl J Med.* 2017;376(25):2415–26.

29. Oldenhuis CN, Oosting SF, Gietema JA, de Vries EG. Prognostic versus predictive value of biomarkers in oncology. *Eur J Cancer*. 2008;44(7):946–53.
30. Hellmann MD, Paz-Ares L, Bernabe Caro R, et al. Nivolumab plus ipilimumab in advanced non-small-cell lung cancer. *N Engl J Med*. 2019;381(21):2020–31.
31. Hellmann MD, Ciuleanu T-E, Pluzanski A, et al. Nivolumab plus ipilimumab in lung cancer with a high tumor mutational burden. *N Engl J Med*. 2018;378(22):2093–104.
32. Harrell FE Jr, Lee KL, Mark DB. Multivariable prognostic models: issues in developing models, evaluating assumptions and adequacy, and measuring and reducing errors. *Stat Med*. 1996;15(4):361–87.
33. Allison A, White IR, Bond S. rpsftm: an R package for rank preserving structural failure time models. *R J*. 2017;9(2):342–53.
34. Gao Z, Hastie T, Tibshirani R. Assessment of heterogeneous treatment effect estimation accuracy via matching. *Stat Med*. 2021;40(17):3990–4013.
35. Schuler A, Baiocchi M, Tibshirani R, Shah N. A comparison of methods for model selection when estimating individual treatment effects. *arXiv*. 2018. <https://doi.org/10.48550/arXiv.1804.05146>.
36. Kaufman JM, Yamada T, Park K, Timmers CD, Amann JM, Carbone DP. A transcriptional signature identifies LKB1 functional status as a novel determinant of MEK sensitivity in lung adenocarcinoma. *Cancer Res*. 2017;77(1):153–63.
37. Hodi FS, Wolchok JD, Schadendorf D, et al. TMB and inflammatory gene expression associated with clinical outcomes following immunotherapy in advanced melanoma. *Cancer Immunol Res*. 2021;9(10):1202–13.
38. Ricciuti B, Wang X, Alessi JV, et al. Association of high tumor mutation burden in non-small cell lung cancers with increased immune infiltration and improved clinical outcomes of PD-L1 blockade across PD-L1 expression levels. *JAMA Oncol*. 2022;8(8):1160–8.
39. Blank CU, Haanen JB, Ribas A, Schumacher TN. Cancer Immunology. The “cancer immunogram.” *Science*. 2016;352(6286):658–60.
40. Rieder D, Fotakis G, Ausserhofer M, et al. nextNEOpI: a comprehensive pipeline for computational neoantigen prediction. *Bioinformatics*. 2021;38:1131–2.
41. Chen Z, Fillmore CM, Hammerman PS, Kim CF, Wong K-K. Non-small-cell lung cancers: a heterogeneous set of diseases. *Nat Rev Cancer*. 2014;14(8):535–46.
42. Ettinger DS, Wood DE, Aisner DL, et al. Non-Small Cell Lung Cancer, Version 3.2022, NCCN Clinical Practice Guidelines in Oncology. *J Natl Compr Canc Netw*. 2022;20(5):497–530.
43. Lapuente-Santana O, van Genderen M, Hilbers PAJ, Finotello F, Eduati F. Interpretable systems biomarkers predict response to immune-checkpoint inhibitors. *Patterns*. 2021;2(8): 100293.
44. Finotello F, Mayer C, Plattner C, et al. Molecular and pharmacological modulators of the tumor immune contexture revealed by deconvolution of RNA-seq data. *Genome Med*. 2019;11(1):34.
45. Schubert M, Klinger B, Klunemann M, et al. Perturbation-response genes reveal signaling footprints in cancer gene expression. *Nat Commun*. 2018;9(1):20.
46. Garcia-Alonso L, Iorio F, Matchan A, et al. Transcription factor activities enhance markers of drug sensitivity in cancer. *Cancer Res*. 2018;78(3):769–80.
47. Kaufman JM, Amann JM, Park K, et al. LKB1 Loss induces characteristic patterns of gene expression in human tumors associated with NRF2 activation and attenuation of PI3K-AKT. *J Thorac Oncol*. 2014;9(6):794–804.
48. Lei M, Siemers NO, Pandya D, et al. Analyses of PD-L1 and inflammatory gene expression association with efficacy of nivolumab +/- ipilimumab in gastric cancer/gastroesophageal junction cancer. *Clin Cancer Res*. 2021;27(14):3926–35.
49. Halkola AS, Joki K, Mirtti T, Mäkelä MM, Aittokallio T, Laajala TD. OSCAR: Optimal subset cardinality regression using the L0-pseudonorm with applications to prognostic modelling of prostate cancer. *bioRxiv* [Internet]. 2022. <https://www.biorxiv.org/content/biorxiv/early/2022/07/02/2022.06.29.498064.full.pdf>.
50. Laajala TD, Joki K, Halkola AS. oscar: Optimal Subset Cardinality Regression (OSCAR) models using the L0-pseudonorm. 2022. <https://CRAN.R-project.org/package=oscar> August 2022.
51. Miller LD, Chou JA, Black MA, et al. Immunogenic subtypes of breast cancer delineated by gene classifiers of immune responsiveness. *Cancer Immunol Res*. 2016;4(7):600–10.
52. Frattini V, Pagnotta SM, Tala, et al. A metabolic function of FGFR3-TACC3 gene fusions in cancer. *Nature*. 2018;553(7687):222–7.
53. Aran D, Hu Z, Butte AJ. xCell: digitally portraying the tissue cellular heterogeneity landscape. *Genome Biol*. 2017;18(1):220.

## Publisher's Note

Springer Nature remains neutral with regard to jurisdictional claims in published maps and institutional affiliations.